

Enzyme-less DNA base identification by chemical stepping in a nanopore

Yujia Qing*, Hagan Bayley

Department of Chemistry, University of Oxford, 12 Mansfield Road, Oxford OX1 3TA, UK

E-mail: yujia.qing@chem.ox.ac.uk

ABSTRACT: The stepwise movement of a single biopolymer strand through a nanoscopic detector for the sequential identification of its building blocks offers a universal means for single-molecule sequencing. This principle has been implemented in portable sequencers that use enzymes to move DNA or RNA through hundreds of individual nanopore detectors positioned in an array. Nevertheless, its application to the sequencing of other biopolymers, including polypeptides and polysaccharides, has not progressed because suitable enzymes are lacking. Recently, we devised a purely chemical means to move molecules processively in steps comparable to the repeat distances in biopolymers. Here, with this chemical approach, we demonstrate sequential nucleobase identification during DNA translocation through a nanopore. Further, the relative location of a guanine modification with a chemotherapeutic platinum derivative is pinpointed with single-base resolution. After further development, chemical translocation might replace stepping by enzymes for highly parallel single-molecule biopolymer sequencing.

Introduction

Nanopore sequencing identifies nucleobases by decoding the changes in an ionic current as a DNA or RNA strand traverses a pore.¹ The translocation is mediated by an enzyme, such as a helicase, to allow the signal to be recorded after the movement of each base. The base-calling fidelity has been perfected over the past decade, lately by the use of machine learning (ML) and synergistic reading heads.^{2,3} The success with nucleic acids is stimulating work on the sequencing of other functional and information-rich biopolymers^{4,5} by the nanopore approach and consequently, a search for suitable devices to control translocation. For example, a biological motor protein has been repurposed to slow down polypeptide translocation⁶ with a step size of 1-4 nm.⁷⁻⁹ At the same time, there have been endeavours to increase sequencing throughput without compromising portability. For example, ionic currents can be converted to fluorescence signals for parallel optical recording, so far with a limited number of pores.^{10,11}

We have devised a chemical means to control the translocation of biopolymers under nano-confinement.¹² The chemical system has the potential to function on a 2D surface and we envision a universal sequencing platform for biopolymers by massively parallel chemical stepping on a chip. The mobile molecule we developed, termed a 'hopper',¹² makes sub-nanometer steps along a track while carrying a strand of biopolymer (Figure 1). The reported prototype translocated an oligo-adenosine sequence by hopping along a series of cysteine footholds, which were evenly spaced on a β strand within the α -hemolysin (α HL) pore. The hops were accomplished through consecutive thiol-disulfide interchange reactions under a transmembrane potential (Figure 1a). The strict regioselectivity of each stepping reaction kept the hopper bound to the track at all times while it moved with high processivity and directionality.^{12,13} While the underlying mechanism of molecular motion has been extensively studied,^{12,13} it has not been demonstrated whether chemical translocation can unravel sequence information in a way

analogous to its enzymatic counterpart. Although the chemical stepper might be used with other biopolymers, DNA is the ideal substrate with which to test sequencing potential; DNA has a uniform distribution of charge along its backbone and there is abundant literature on its unassisted^{14,15} and enzyme-facilitated translocation through nanopores.¹⁶⁻¹⁸ Here, we demonstrate single-nucleotide discrimination and the sequential identification of natural and modified nucleobases during stepwise chemical translocation of DNA through a nanopore.

Results and Discussion

DNA sequences of interest were prepared as conjugates with a traptavidin-capped peptide carrier through a disulfide linkage (Figure 1 and Figure S1). To initiate DNA translocation by chemical stepping, a DNA-peptide conjugate was first threaded from the cis side into a protein nanopore with a five-cysteine track. The terminal traptavidin stopper arrested translocation and the DNA subsequently became covalently attached to the wall of the pore through regioselective thiol-disulfide interchange between a foothold cysteine sidechain and the disulfide linker.¹³ We then applied a transmembrane potential of ± 150 mV to extend and orient the negatively charged DNA within the β barrel, thereby controlling the direction of motion.¹² In this way, the DNA was moved from one end of the track to the other repeatedly. Occasional back-stepping was observed (Figure 1d), because the DNA chain retains conformational lability even under the pulling force and can bend backward to react with the preceding foothold.¹² This is more prominent after the hopper reached the terminal foothold, as no forward footholds remained. The hopper was installed at the 5' end of a DNA strand to move it stepwise outside a nanopore. The ionic current passing through the pore reflected both the position of the hopper within the pore and the sequence of the DNA cargo. The repeated motion allowed us to characterize the same DNA molecule multiple times, which was only limited by bilayer stability. The overall residence time of the DNA hopper was controlled by the small-molecule reducing reagent, 1,4-dithiothreitol (DTT) (1 mM, trans), which cleaved the DNA

from the track after several rounds of translocation. This turnover allowed the examination of one DNA molecule after another.

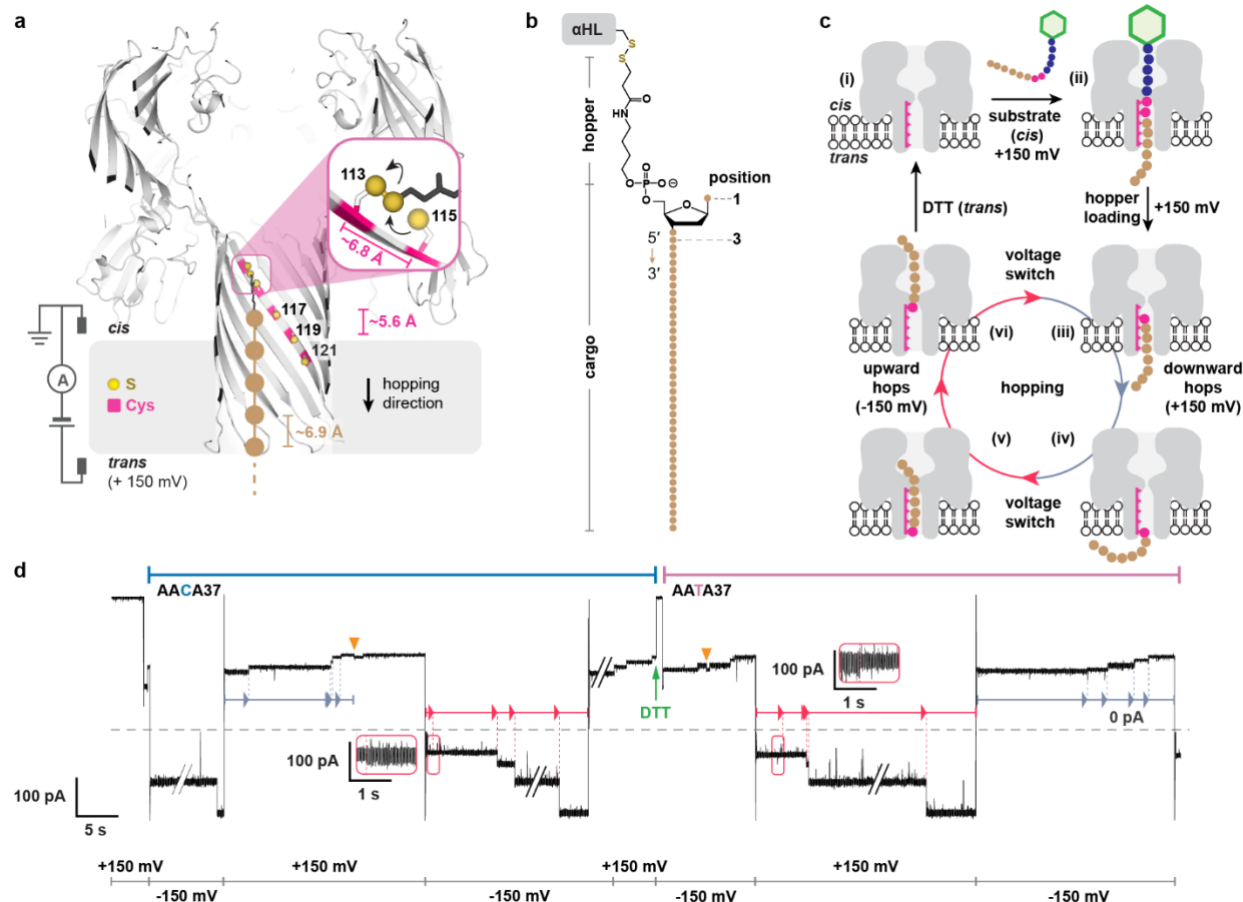


Figure 1. Chemical stepping of oligonucleotides within an α -hemolysin (α HL) pore. **(a)** The molecular hopper (black) carries a single-stranded DNA (brown) and moves along a five-cysteine track (pink) within the β barrel of an engineered α HL pore through consecutive thiol-disulfide interchange reactions. The inset shows a close-up of the regioselective attack of a foothold thiolate on the disulfide linking the molecular hopper to the track, thereby producing a single step. **(b)** The structure of a hopper carrying an oligo-adenosine 40-mer (A40) cargo. **(c)** A molecular hopper carrying a DNA cargo (brown) is added to the solution as a mixed disulfide (S atoms, pink) with a peptide carrier (blue) that is capped by traptavidin (green hexagon) (Figure S1). Under an applied potential (+150 mV, trans), the mixed disulfide threads into the nanopore (i) from the cis side and translocation is arrested by the traptavidin stopper (ii). The ensuing thiol-disulfide interchange between a cysteine thiolate and the mixed disulfide loads the hopper-cargo complex onto the track (iii). The applied potential controls the hopping direction (iv-vi). Reduction of the disulfide linking the hopper with the track by DTT (1 mM in the trans compartment) regenerates the free track within the nanopore (i) ready for the loading of a subsequent hopper. **(d)** With a five-cysteine track, four-step hopping was observed at +150 mV (grey arrows) and -150 mV (red arrows) with a hopper carrying a 40-mer DNA cargo that contained T or C at the third position in an oligo-adenosine background. Occasional back-stepping was observed (orange arrows). The insets zoom in on the transition from Cys-121 to Cys-119 for both sequences under -150 mV. Current traces apart from those in the insets were filtered at 1 kHz. Conditions: 2 M KCl, 50 mM HEPBS, 50 mM EDTA, pH 8.5, $20^\circ \pm 1^\circ\text{C}$

Sequential identification of natural nucleobases by chemical stepping

To demonstrate that chemical stepping facilitated the discrimination of the four natural bases of DNA with single-base resolution, two sets of oligo-adenosine 40-mers were used. One set contained an A, T, C, or G base at the first position and the other set an A, T, C, or G base at the third position (Figure 1d, Figure 2, and Figure S2). Distinct current patterns were recorded for each of these oligonucleotides when they were moved one direction or the other, along the five-cysteine track. The base causing the maximum current blockade varied at different footholds

(Figure 2), which was also observed with the streptavidin-immobilized DNA strands that differ by one base at various positions.¹⁹ The current levels recorded when a single oligonucleotide was read multiple times with the same nanopore were consistent (S.D. <0.5 % at all footholds, Figure S3). The differences in current levels obtained with a particular pore and different DNAs of the same sequence were also negligible (S.D. <0.5%) and minimal across a collection of individual pores (S.D. <1%) (Table S1 and Table S2). The turnover of hopper-cargo complexes with DTT¹³ (1 mM, trans) showed that the sequences of different DNAs could be distinguished with the same pore (Figure 1d).

The presence of sequence information within current traces was supported further by the analysis of a set of four A40 oligo-nucleotides with single C substitutions at positions 1 through 4 (Figure 3, Figure S4 and Figure S5). First, the ‘background’ was corrected by subtracting the Ires% value—the remaining current as a percentage of the open pore current—for the homo-oligomer A40 from the values for the C-substituted oligonucleotides ($\Delta\text{Ires}\% = \text{Ires}\%(\text{AnCA}(39\text{-n})) - \text{Ires}\%(\text{A40})$, $n = 0\text{-}3$) (Figure 3b, Figure S5). Given that the internucleotide distance in a stretched single-stranded DNA (~ 6.9 Å) is similar to the step size of the hopper (~ 5.6 Å) (Figure 1a),¹² the current traces for the four oligonucleotides were then offset step by step (Figure 3c). In this a way, the C base would be approximately at the same site within the pore for each position on the x-axis of

the plot (Figure S5a). The offset plots show an imperfect but readily discernible convergence, especially at +150 mV (Figure 3c) (mean root-mean-square deviation (RMSD) of $\Delta\text{Ires}\%$ (background subtracted) = 2.5%; mean RMSD of $\Delta\text{Ires}\%$ (offset) = 1.0%, Figure S5b). The convergence was especially striking for the three positions where the C base lay closest to the trans entrance (mean RMSD (offset) = 0.5%, Figure S5b). The convergence under -150 mV was less ideal, presumably because the cytosine residues were mostly outside the β barrel (Figure S5a). Given recent advances in ML,^{20,21} it is likely that similar signals could be converted to sequence information. We then moved on to examine individual modified nucleobases by chemical translocation, in which case the single-step offset was directly visible in the current traces.

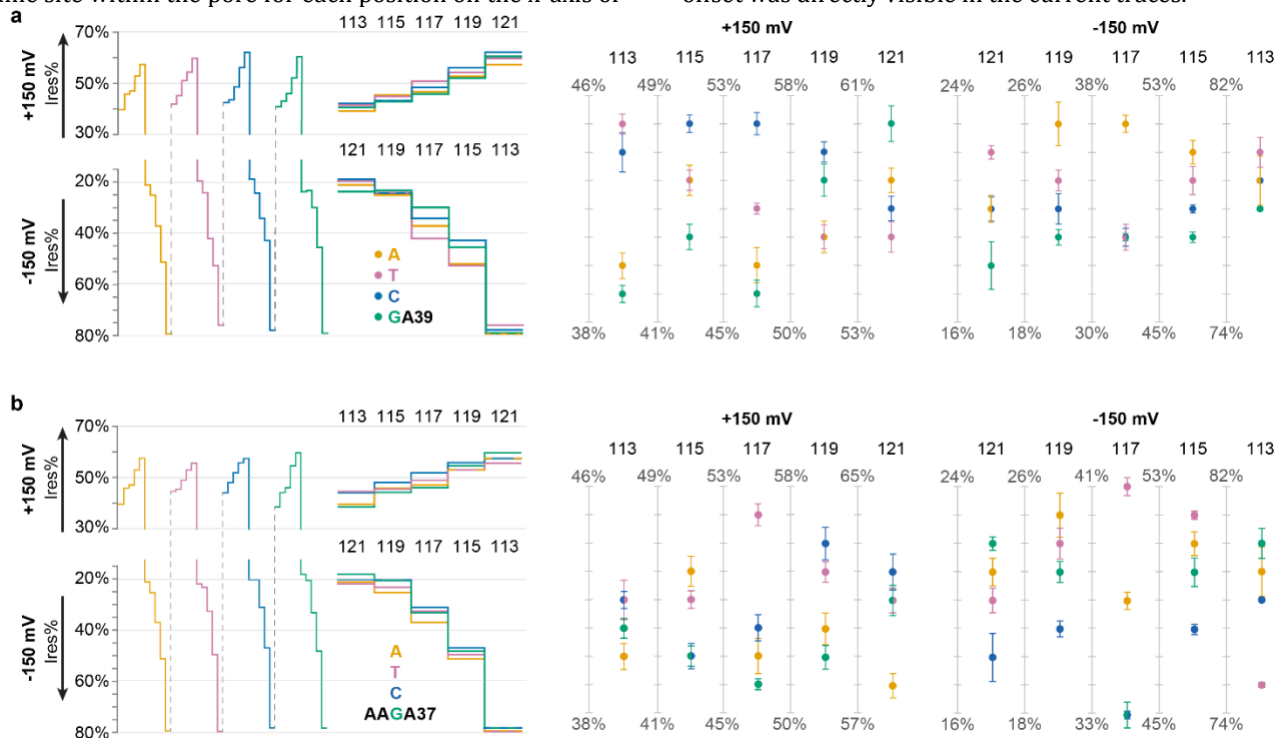


Figure 2. Single-base discrimination of the four DNA bases. Idealised current traces with step durations equalized for the four DNA cargos in a set with A, T, C, or G as the first (a) or the third (b) base. The current levels are given as the mean residual current with respect to the open pore level (Ires%). For each sequence, data were recorded with $n > 3$ separate pores and $n > 3$ molecules of the same sequence with each pore. The errors shown here were derived from different pores, whereas errors in data acquired with the same pore were $< 0.5\%$. All data points are given in Table S1 and Table S2.

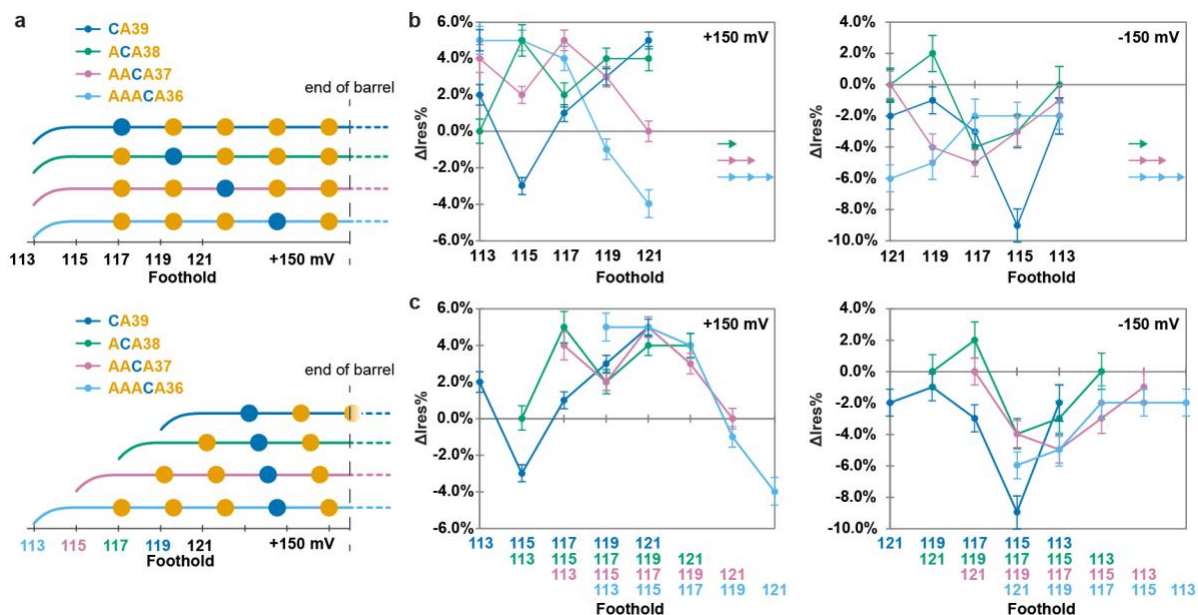


Figure 3. Positional discrimination of a cytosine within an oligo-adenosine DNA. **(a)** Given that the step size of chemical translocation is similar to the inter-nucleotide distance, offsetting the current traces step by step aligns the cytosines of interest to be approximately at the same site within the pore. One example of the expected convergence of C across four tested sequences is shown by step offsetting under +150 mV. **(b)** To eliminate the background of the moving hopper, the residual current ($I_{res}\%$, the remaining current as a percentage of the open pore current) for oligo-adenosine 40-mer was subtracted from the current measured with a C-containing oligonucleotide at each foothold ($\Delta I_{res}\% = I_{res}\%(\text{AnCA}(39-n)) - I_{res}\%(\text{A40})$, $n = 1-4$). To check whether the current differences reflected the offset cytosine positions within the sequences, individual background-free $\Delta I_{res}\%$ plots were offset one step at a time (arrows indicating the number of offsetting steps). The resultant plots **(c)** show an imperfect but readily discernible convergence at ± 150 mV.

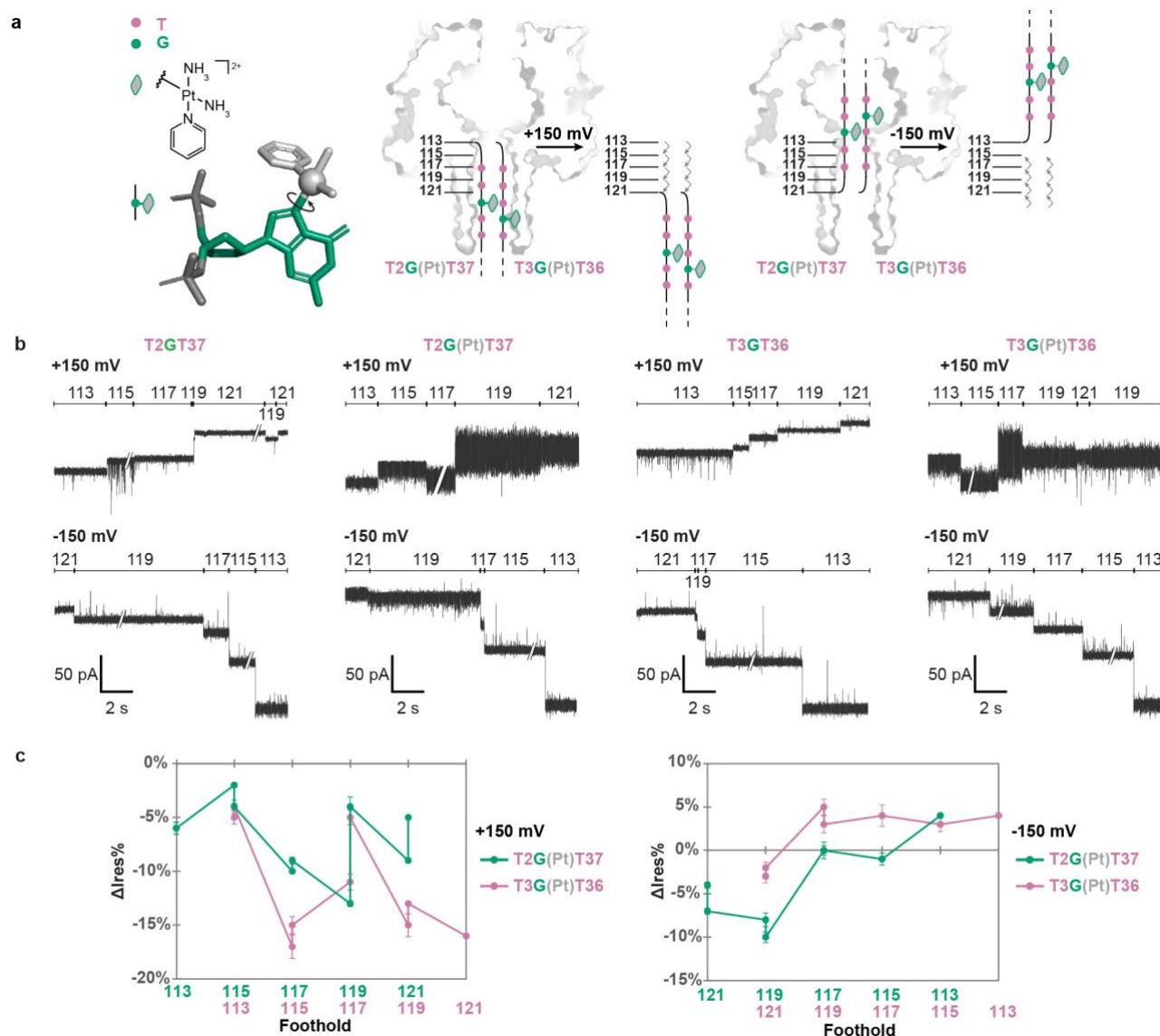


Figure 4. Positional discrimination of the modified bases within platinated DNAs. **(a)** Two oligo-thymidine 40-mer DNAs (red) containing a single guanine nucleotide (green) at the third or fourth position (T2GT37 and T3GT36) were platinated at the guanine site with pyriplatin (pink square) and subjected to sequence characterization by chemical stepping. The displayed structure of pyriplatin bound to guanosine is taken from a pyriplatin-modified DNA duplex (PDB code: 3co3). **(b)** Current traces showing the four-step hopping observed with the unplatinated and the platinated oligonucleotides at ± 150 mV. Current traces were filtered at 1 kHz. Conditions: 2 M KCl, 50 mM HEPBS, 20 mM EDTA, pH 8.5, $20^\circ \pm 1^\circ\text{C}$. **(c)** To eliminate the background of the moving hopper, the residual current (Ires%) for the oligo-thymidine 40-mer containing a single guanosine was subtracted from the current measured after a pyriplatin modification at each foothold ($\Delta I_{res}\% = I_{res}\%(\text{T2G(Pt)T37}) - I_{res}\%(\text{T2GT37})$ or $I_{res}\%(\text{T3G(Pt)T36}) - I_{res}\%(\text{T3GT36})$). To determine whether the current differences reflected the pyriplatin positions that are offset by one base, individual background-subtracted $\Delta I_{res}\%$ plots were offset by one step. The resulting plots show an obvious convergence at ± 150 mV (Figure S7)

Sequential identification of modified nucleobases by chemical stepping

Platinum drugs are used for cancer chemotherapy.^{22,23} Nucleobase modification with platinum drugs has been associated with the inhibition of transcription, which leads to cancer cell death.^{22,23} While clinically approved bifunctional platinum complexes (e.g. cisplatin) crosslink purine bases on the same DNA strand or different strands,²⁴ an emergent class of platinum complexes form monovalent adducts on the N7 of guanosine residues with minimal perturbation to the duplex structure.²⁵ The monofunctional platinum agents (e.g. pyriplatin and phenanthriplatin) differ from the bifunctional agents in their spectrum of

activity against human cancer cell lines.^{26,27} Therefore, further studies on their mechanism of action would be desirable. Considerable effort has been put into the identification of platination sites of bifunctional platinum drugs on DNA by biochemical means^{22,23} and more recently by next-generation sequencing with the aid of affinity-based sequence enrichment.^{28,29} For DNA lesions, PCR amplification is precluded and single-molecule nanopore sequencing offers a label-free and amplification-free alternative with single-nucleotide resolution. To move a DNA strand through a lesion site for sequencing, we could either engineer the enzyme to step over the obstacle or apply a universal chemical stepper—the molecular hopper.

Here, we applied chemical stepping to characterize oligonucleotides modified by the monofunctional anticancer agent pyriplatin.^{25–27} Two 40-mer oligothymidine sequences containing a single guanosine at adjacent positions (T2GT37 and T3GT36) were platinated (T2G(Pt)T37 and T3G(Pt)T36) and moved stepwise through the nanopore (Figure 4a). We recorded significantly ‘noisier’ current traces with both sequences when they resided at any of the five footholds under +150 mV, and with T2G(Pt)T37 at Cys-121 and Cys-119, and with T3G(Pt)T37 at Cys-121, under -150 mV (Figure 4b). The ‘noise’ occurred when the platinum complex was expected to be within the β barrel of the pore during DNA translocation (Figure 4a). For both sequences, the current noise clearly resolved into at least two interconverting levels for Cys-115 and Cys-117 at +150 mV and for Cys-119 and Cys-121 at ± 150 mV (Figure S6 and Figure S7), which has been observed previously with conformationally labile small molecules.³⁰ Indeed, NMR study of small-molecule models of phenanthriplatin-DNA complex revealed two conformational diastereomers that rapidly interconvert via rotation about the Pt-N_{phenanthriplatin} bond.³¹ Similarly, a pyriplatin-guanosine complex might have interconvertible rotamers, to which we attribute the recorded ‘noise’ in current. We noted a one-step offset in current patterns between the two platinated sequences, again more pronounced at +150 mV (Figure 4c and Figure S7), which is in keeping with the one-nucleotide offset in the platination sites. Although a platinum complex was registered by a characteristic ionic current at the threading stage prior to the stepping motion (Figure S8), the platination site was more clearly resolved out when the DNA was moved base-by-base through the nanopore detector.

Conclusion

In summary, we have demonstrated sequential DNA base identification by chemical stepping using a nanopore platform in a proof-of-concept study. DNA sequences that differ by one base in either identity or position have been unambiguously discriminated by their current signatures. Further, we have established that moving DNA by our chemical approach provides positional information of a single base, being natural or modified, which is unattainable by static sensing. Although we cannot yet translate the current patterns into exact sequences, it is likely to be achieved with ML algorithms trained with extensive datasets. Indeed, early work using enzymatic translocation produced current ‘squiggles’ that were only later fully decoded into sequences with advanced basecalling tools.¹ One of the advantages of chemical stepping is the ability to read a single DNA molecule multiple times. In addition, we have incorporated a turnover mechanism so that multiple molecules of either the same sequence or different sequences can be read with the same nanopore, each one repeatedly. This is the first enzyme-free strategy which might be applied to biopolymers other than DNA. Take polypeptides for example, this stepping chemistry will move ~ 1.6 amino acids per step, while no known enzymes step one amino acid at a time. For future work, it is interesting to consider the step size in the context of sequencing. We envision that the step size (D_{step}) has to be comparable to the distance between the building blocks of biopolymers (D_{bb}) to ensure full coverage of sequence information. It cannot be too big (e.g., $D_{\text{step}} \gg 20D_{\text{bb}}$) as

information will be lost in every step forward; it can be smaller than the building blocks (e.g., $D_{\text{step}} \sim 0.8D_{\text{bb}}$) so that each building block is ‘read’ more than once; it can be slightly larger (e.g., $D_{\text{step}} \sim 1.5D_{\text{bb}}$) as a reading head is likely to register several building blocks at once.

Although the limited read length offered by a protein nanopore platform might be useful for less demanding tasks such as protein identification, the future realization of biopolymer sequencing by chemical stepping requires tracks of hundreds of steps. To tackle this issue, the stepping chemistry might be effected on an extended surface with precisely spaced footholds. For example, the surface of crystalline cadmium sulphide displays sulfur atoms separated by $\sim 4.1 \text{ \AA}^{32}$ —a favourable spacing for biopolymer sequencing. With a track length of 500 nm, we could cover a DNA strand of >700 bases, or a polypeptide chain of >1000 amino acids. Moreover, ~ 1 million tracks of such length might be accommodated on a $2 \times 2 \text{ }\mu\text{m}$ microchip for parallel sequencing. Such a process would encounter serious challenges, which include the directional control of chemical stepping on a surface, possibly by applying flow, and parallel molecular detection at engineered sites along individual tracks, perhaps through tunnelling currents.^{33,34} Nonetheless, chemical stepping for the sequential identification of building blocks is a significant step towards a universal ultra-high throughput sequencing technology for biopolymers.

ASSOCIATED CONTENT

Supporting Information.

Figures S1–S10 and Tables S1–S3; Experimental procedures and characterization data.

AUTHOR INFORMATION

Corresponding Author

Yujia Qing – Chemistry research laboratory, 12 Mansfield road, Oxford, OX1 3TA, U.K.; orcid.org/0000-0002-2110-4269; Email: yujia.qing@chem.ox.ac.uk

Author

Hagan Bayley – Chemistry research laboratory, 12 Mansfield road, Oxford, OX1 3TA, U.K.; orcid.org/0000-0003-2499-6116

Funding Sources

This research was supported by Oxford Nanopore Technologies and a European Research Council Advanced Grant (SYNTISU). Y.Q. is supported by a Glasstone Research Fellowship and a Fellowship by Examination, Magdalen College, Oxford.

ACKNOWLEDGMENT

We thank Guangyu Zhu and Fang Wang for their suggestions on DNA modification with pyriplatin.

ABBREVIATIONS

ML, machine learning; αHL , α -hemolysin; DTT, 1,4-dithiothreitol; RMSD, mean root-mean-square deviation.

REFERENCES

- (1) Bayley, H. Nanopore Sequencing: From Imagination to Reality. *Clin. Chem.* **2015**, *61* (1), 25–31.
- (2) Van der Verren, S. E.; Van Gerven, N.; Jonckheere, W.;

- Hambley, R.; Singh, P.; Kilgour, J.; Jordan, M.; Wallace, E. J.; Jayasinghe, L.; Remaut, H. A Dual-Constriction Biological Nanopore Resolves Homonucleotide Sequences with High Fidelity. *Nat. Biotechnol.* **2020**, *38* (12), 1415–1420.
- (3) Stoddart, D.; Maglia, G.; Mikhailova, E.; Heron, A. J.; Bayley, H. Multiple Base-Recognition Sites in a Biological Nanopore: Two Heads Are Better than One. *Angew. Chem. Int. Ed.* **2010**, *49*, 556–559.
- (4) Restrepo-Pérez, L.; Joo, C.; Dekker, C. Paving the Way to Single-Molecule Protein Sequencing. *Nat. Nanotechnol.* **2018**, *13* (9), 786–796.
- (5) Alfaro, J. A.; Bohländer, P.; Dai, M.; Filius, M.; Howard, C. J.; van Kooten, X. F.; Ohayon, S.; Pomorski, A.; Schmid, S.; Aksimentiev, A.; Anslyn, E. V.; Bedran, G.; Cao, C.; Chinappi, M.; Coyaoud, E.; Dekker, C.; Dittmar, G.; Drachman, N.; Eelkema, R.; Goodlett, D.; Hentz, S.; Kalathiya, U.; Kelleher, N. L.; Kelly, R. T.; Kelman, Z.; Kim, S. H.; Kuster, B.; Rodriguez-Larrea, D.; Lindsay, S.; Maglia, G.; Marcotte, E. M.; Marino, J. P.; Masselon, C.; Mayer, M.; Samaras, P.; Sarthak, K.; Sepiashvili, L.; Stein, D.; Wanunu, M.; Wilhelm, M.; Yin, P.; Meller, A.; Joo, C. The Emerging Landscape of Single-Molecule Protein Sequencing Technologies. *Nat. Methods* **2021**, *18* (6), 604–617.
- (6) Nivala, J.; Marks, D. B.; Akeson, M. Unfoldase-Mediated Protein Translocation through an α -Hemolysin Nanopore. *Nat. Biotechnol.* **2013**, *31* (3), 247–250.
- (7) Maillard, R. A.; Chistol, G.; Sen, M.; Righini, M.; Tan, J.; Kaiser, C. M.; Hodges, C.; Martin, A.; Bustamante, C. ClpX(P) Generates Mechanical Force to Unfold and Translocate Its Protein Substrates. *Cell* **2011**, *145* (3), 459–469.
- (8) Aubin-Tam, M. E.; Olivares, A. O.; Sauer, R. T.; Baker, T. A.; Lang, M. J. Single-Molecule Protein Unfolding and Translocation by an ATP-Fueled Proteolytic Machine. *Cell* **2011**, *145* (2), 257–267.
- (9) Sen, M.; Maillard, R. A.; Nyquist, K.; Rodriguez-Aliaga, P.; Pressé, S.; Martin, A.; Bustamante, C. The ClpXP Protease Unfolds Substrates Using a Constant Rate of Pulling but Different Gears. *Cell* **2013**, *155* (3), 636–646.
- (10) Huang, S.; Romero-Ruiz, M.; Castell, O. K.; Bayley, H.; Wallace, M. I. High-Throughput Optical Sensing of Nucleic Acids in a Nanopore Array. *Nat. Nanotechnol.* **2015**, *10* (11), 986–991.
- (11) Wang, Y.; Wang, Y.; Du, X.; Yan, S.; Zhang, P.; Chen, H.-Y.; Huang, S. Electrode-Free Nanopore Sensing by DiffusiOptoPhysiology. *Sci. Adv.* **2019**, *5* (9), eaar3309.
- (12) Qing, Y.; Ionescu, S. A.; Pulcu, G. S.; Bayley, H. Directional Control of a Processive Molecular Hopper. *Science* **2018**, *361* (6405), 908–912.
- (13) Qing, Y.; Tamagaki-Asahina, H.; Ionescu, S. A.; Liu, M. D.; Bayley, H. Catalytic Site-Selective Substrate Processing within a Tubular Nanoreactor. *Nat. Nanotechnol.* **2019**, *14* (12), 1135–1142.
- (14) Kasianowicz, J. J.; Brandin, E.; Branton, D.; Deamer, D. W. Characterization of Individual Polynucleotide Molecules Using a Membrane Channel. *Proc. Natl. Acad. Sci. U. S. A.* **1996**, *93* (24), 13770–13773.
- (15) Maglia, G.; Restrepo, M. R.; Mikhailova, E.; Bayley, H. Enhanced Translocation of Single DNA Molecules through α -Hemolysin Nanopores by Manipulation of Internal Charge. *Proc. Natl. Acad. Sci. U. S. A.* **2008**, *105* (50), 19720–19725.
- (16) Cherf, G. M.; Lieberman, K. R.; Rashid, H.; Lam, C. E.; Karplus, K.; Akeson, M. Automated Forward and Reverse Ratcheting of DNA in a Nanopore at 5-Å Precision. *Nat. Biotechnol.* **2012**, *30* (4), 344–348.
- (17) Olasagasti, F.; Lieberman, K. R.; Benner, S.; Cherf, G. M.; Dahl, J. M.; Deamer, D. W.; Akeson, M. Replication of Individual DNA Molecules under Electronic Control Using a Protein Nanopore. *Nat. Nanotechnol.* **2010**, *5* (11), 798–806.
- (18) Akeson, M.; Branton, D.; Kasianowicz, J. J.; Brandin, E.; Deamer, D. W. Microsecond Time-Scale Discrimination among Polycytidylic Acid, Polyadenylic Acid, and Polyuridylic Acid as Homopolymers or as Segments within Single RNA Molecules. *Biophys. J.* **1999**, *77* (6), 3227–3233.
- (19) Stoddart, D.; Heron, A. J.; Mikhailova, E.; Maglia, G.; Bayley, H. Single-Nucleotide Discrimination in Immobilized DNA Oligonucleotides with a Biological Nanopore. *Proc. Natl. Acad. Sci. U. S. A.* **2009**, *106*, 7702–7707.
- (20) Silver, D.; Hubert, T.; Schrittwieser, J.; Antonoglou, I.; Lai, M.; Guez, A.; Lanctot, M.; Sifre, L.; Kumaran, D.; Graepel, T.; Lillicrap, T.; Simonyan, K.; Hassabis, D. A General Reinforcement Learning Algorithm That Masters Chess, Shogi, and Go through Self-Play. *Science* **2018**, *362* (6419), 1140–1144.
- (21) Senior, A. W.; Evans, R.; Jumper, J.; Kirkpatrick, J.; Sifre, L.; Green, T.; Qin, C.; Židek, A.; Nelson, A. W. R.; Bridgland, A.; Penedones, H.; Petersen, S.; Simonyan, K.; Crossan, S.; Kohli, P.; Jones, D. T.; Silver, D.; Kavukcuoglu, K.; Hassabis, D. Improved Protein Structure Prediction Using Potentials from Deep Learning. *Nature* **2020**, *577* (7792), 706–710.
- (22) Johnstone, T. C.; Suntharalingam, K.; Lippard, S. J. The next Generation of Platinum Drugs: Targeted Pt(II) Agents, Nanoparticle Delivery, and Pt(IV) Prodrugs. *Chem. Rev.* **2016**, *116* (5), 3436–3486.
- (23) Jamieson, E. R.; Lippard, S. J. Structure, Recognition, and Processing of Cisplatin–DNA Adducts. *Chem. Rev.* **1999**, *99* (9), 2467–2498.
- (24) Fichtinger-Schepman, A. M. J.; Van der Veer, J. L.; Den Hartog, J. H. J.; Lohman, P. H. M.; Reedijk, J. Adducts of the Antitumor Drug Cis-Diamminedichloroplatinum(II) with DNA: Formation, Identification, and Quantitation. *Biochemistry* **1985**, *24* (3), 707–713.
- (25) Lovejoy, K. S.; Todd, R. C.; Zhang, S.; McCormick, M. S.; D'Aquino, J. A.; Reardon, J. T.; Sancar, A.; Giacomini, K. M.; Lippard, S. J. Cis-Diammine(Pyridine)Chloroplatinum(II), a Monofunctional Platinum(II) Antitumor Agent: Uptake, Structure, Function, and Prospects. *Proc. Natl. Acad. Sci. U. S. A.* **2008**, *105* (26), 8902–8907.
- (26) Zhu, G.; Myint, M.; Ang, W. H.; Song, L.; Lippard, S. J. Monofunctional Platinum–DNA Adducts Are Strong Inhibitors of Transcription and Substrates for

- Nucleotide Excision Repair in Live Mammalian Cells. *Cancer Res.* **2012**, 72 (3), 790–800.
- (27) Lovejoy, K. S.; Serova, M.; Bieche, I.; Emami, S.; D’Incalci, M.; Broggin, M.; Erba, E.; Gespach, C.; Cvitkovic, E.; Faivre, S.; Raymond, E.; Lippard, S. J. Spectrum of Cellular Responses to Pyriplatin, a Monofunctional Cationic Antineoplastic Platinum(II) Compound, in Human Cancer Cells. *Mol. Cancer Ther.* **2011**, 10 (9), 1709–1719.
- (28) Shu, X.; Xiong, X.; Song, J.; He, C.; Yi, C. Base-Resolution Analysis of Cisplatin-DNA Adducts at the Genome Scale. *Angew. Chem. Int. Ed.* **2016**, 128 (46), 14458–14461.
- (29) Hu, J.; Lieb, J. D.; Sancar, A.; Adar, S. Cisplatin DNA Damage and Repair Maps of the Human Genome at Single-Nucleotide Resolution. *Proc. Natl. Acad. Sci. U. S. A.* **2016**, 113 (41), 11507–11512.
- (30) Qing, Y.; Liu, M. D.; Hartmann, D.; Zhou, L.; Ramsay, W. J.; Bayley, H. Single-Molecule Observation of Intermediates in Bioorthogonal 2-Cyanobenzothiazole Chemistry. *Angew. Chem. Int. Ed.* **2020**, 59 (36), 15711–15716.
- (31) Johnstone, T. C.; Lippard, S. J. The Chiral Potential of Phenanthriplatin and Its Influence on Guanine Binding. *J. Am. Chem. Soc.* **2014**, 136 (5), 2126–2134.
- (32) Sadovnikov, S. I.; Rempel, A. A.; Gusev, A. I. Nanostructured Cadmium Sulfide CdS. In *Nanostructured Lead, Cadmium, and Silver Sulfides: Structure, Nonstoichiometry and Properties*; Springer Series in Materials Science; Springer International Publishing: Cham, 2018; Vol. 256, pp 127–188.
- (33) Huang, S.; He, J.; Chang, S.; Zhang, P.; Liang, F.; Li, S.; Tuchband, M.; Fuhrmann, A.; Ros, R.; Lindsay, S. Identifying Single Bases in a DNA Oligomer with Electron Tunnelling. *Nat. Nanotechnol.* **2010**, 5 (12), 868–873.
- (34) Tanaka, H.; Kawai, T. Partial Sequencing of a Single DNA Molecule with a Scanning Tunnelling Microscope. *Nat. Nanotechnol.* **2009**, 4 (8), 518–522.

